Atomic four-level *N* systems

C. Goren,[1] A. D. Wilson-Gordon,[2] M. Rosenbluh,[1] and H. Friedmann[2]
[1]*Department of Physics, Bar-Ilan University, Ramat Gan 52900, Israel*
[2]*Department of Chemistry, Bar-Ilan University, Ramat Gan 52900, Israel*
(Received 14 January 2004; published 26 May 2004)

We investigate the atomic four-level *N* configuration both analytically and numerically, for various pump and probe intensities, with and without transfer of coherence (TOC) and Doppler broadening, and compare the results obtained to those of realistic atomic systems. We find that TOC affects the whole spectrum, in addition to producing an electromagnetically induced absorption (EIA) peak at line center. We show that the EIA peak splits as the pump intensity increases. These results are compared with those of realistic systems. When the pump is σ^+ polarized and the probe is π polarized, the results are similar to those of the *N* configuration. When the pump and probe polarizations are both linear with perpendicular polarizations, various *N*-like subsystems contribute to the spectrum. Consequently, the splitting of the EIA peak only occurs at very high pump intensities. We also discuss the influence of the probe on the pump absorption and refraction and find that both the pump and probe show EIA peaks when the pump intensity is low, and complementary behavior when the pump is intense. At both low and high pump intensity, the pump and probe dispersions are of opposite sign.

DOI: 10.1103/PhysRevA.69.053818 PACS number(s): 42.50.Gy, 42.50.Nn, 42.65.−k

I. INTRODUCTION

The phenomenon of electromagnetically induced absorption (EIA) in degenerate two-level atomic systems has been the focus of many theoretical and experimental [1–6] papers. The simplest model that produces EIA is the four-level *N* system (see Fig. 1), provided that the analysis includes transfer of excited state coherence via spontaneous emission to ground state coherence [7,8]. In a recent publication [9], we rationalized the experimental conditions needed to observe EIA due to transfer of coherence (TOC), namely the requirements that $F_g>0$, $F_e=F_g+1$ and that the pump and probe lasers have different polarizations. In addition, we proposed [9] a new type of EIA due to transfer of population (TOP) that occurs when the pump and probe have the same polarizations.

In this paper, we present a full analytical and numerical study of the *N* configuration atom and compare the results obtained with those of realistic degenerate two-level systems. When TOC is included, the *N* configuration corresponds to the situation where a degenerate two-level transition, with $F_e=F_g+1$ and $F_g>0$, is pumped by a resonant σ^+ polarized pump laser and probed by a tunable weak π polarized probe laser. The absence of TOC corresponds to an *N* configuration where the transitions are far from degenerate, as in the Na_2 molecular system discussed by Dong *et al.* [10]. Previous theoretical work on the *N* system, in which EIA was obtained [7,8], was limited to low pump intensity and even lower probe intensity. Dips in the EIA spectrum due to Doppler broadening were predicted by Taichenachev *et al.* [8] using the *N* configuration and observed by Kim *et al.* [6]. Here we show that such dips can be obtained even in the absence of Doppler broadening at high pump intensity. We compare the full absorption spectra obtained in the absence [10] and the presence of TOC, when Doppler broadening is either included or excluded.

Another topic explored in this paper is the effect of a moderately intense probe on the pump absorption and refraction. We find that when the pump is sufficiently weak, both the pump and probe absorption spectra are characterized by enhanced absorption. However, the probe and pump dispersions are of opposite sign, negative for the probe [11] and positive for the pump. When the pump intensity is high, the pump and probe absorption while both positive, exhibit opposite behavior (that is, when the pump absorption increases, that of the probe decreases, and vice versa). Such behavior of the absorption spectrum has also been found for the simple two-level system [12]. At line center, the pump and probe dispersions are also opposites, positive for the probe and negative for the pump.

Finally, we compare the results of the *N* configuration to those obtained using degenerate two-level transitions of real alkali atoms, with $F_e=F_g+1$ and $F_g>0$. Two cases are considered: in the first, the transition interacts with a σ^+ polarized pump and a tunable weak π polarized probe (similar to the *N* configuration) and in the second, the pump and probe are both linearly polarized but have perpendicular polarizations. The latter case can be thought of as a combination of *N*-like systems.

II. *N*-LEVEL ATOM

A. Equations of motion

The four-state *N* configuration (see Fig. 1) including TOC, has been used in the limit of low pump intensity [7,8] as a model for predicting EIA. In this scheme two pump

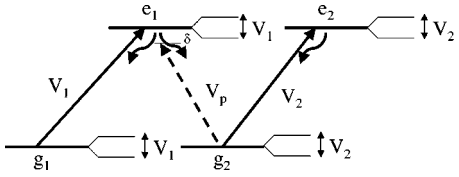

FIG. 1. Energy level scheme for the four-level *N* configuration atom interacting with two resonant pumps, V_1 and V_2 and a tunable probe, V_p.

lasers, with Rabi frequencies V_1 and V_2, couple levels g_1 to e_1 and g_2 to e_2, respectively. A probe laser with Rabi frequency V_p couples level g_2 to e_1. The e_2 to g_1 transition is forbidden by selection rules. We begin by writing the Bloch equations for the N configuration in the rotating-wave approximation. The off-diagonal density matrix elements $\rho_{e_ie_j}$, $\rho_{e_ig_j}$, and $\rho_{g_ig_j}$, where $(i,j)=(1,2)$ can be written in terms of their Fourier amplitudes as

$$\rho_{e_ig_i} = \rho_{e_ig_i}(\omega_i)\exp(-i\omega_i t), \tag{1}$$

$$\rho_{e_1g_2} = \rho_{e_1g_2}(\omega_p)\exp(-i\omega_p t), \tag{2}$$

$$\rho_{e_2g_1} = \rho_{e_1e_2}(\omega_1+\omega_2-\omega_p)\exp[-i(\omega_1+\omega_2-\omega_p)t], \tag{3}$$

$$\rho_{e_1e_2} = \rho_{e_1e_2}(\omega_p-\omega_2)\exp[-i(\omega_p-\omega_2)t], \tag{4}$$

$$\rho_{g_1g_2} = \rho_{g_1g_2}(\omega_p-\omega_1)\exp[-i(\omega_p-\omega_1)t]. \tag{5}$$

The following set of linear equations for the Fourier amplitudes to all orders in V_1 V_2, and V_p are then obtained:

$$\dot{\rho}_{g_1g_1} = A^2\Gamma\rho_{e_1e_1} - i[V_1\rho_{g_1e_1}(-\omega_1) - V_1^*\rho_{e_1g_1}(\omega_1)] - \gamma(\rho_{g_1g_1}-\rho_{g_1g_1}^{eq}), \tag{6}$$

$$\dot{\rho}_{g_2g_2} = (B^2\rho_{e_1e_1}+\rho_{e_2e_2})\Gamma - \gamma(\rho_{g_2g_2}-\rho_{g_2g_2}^{eq}) - i[V_p\rho_{g_2e_1}(-\omega_p) - V_p^*\rho_{e_1g_2}(\omega_p) + V_2\rho_{g_2e_2}(-\omega_2) - V_2^*\rho_{e_2g_2}(\omega_2)], \tag{7}$$

$$\dot{\rho}_{g_1g_2}(\omega_p-\omega_1) = -[i(\Delta_p-\Delta_1)+\gamma]\rho_{g_1g_2}(\omega_p-\omega_1) - i[V_p\rho_{g_1e_1}(-\omega_1) + V_2\rho_{g_1e_2}(\omega_p-\omega_1-\omega_2) - V_1^*\rho_{e_1g_2}(\omega_p)] + bA\Gamma\rho_{e_1e_2}(\omega_p-\omega_1), \tag{8}$$

$$\dot{\rho}_{e_1g_1}(\omega_1) = -(i\Delta_1+\Gamma/2+\gamma)\rho_{e_1g_1}(\omega_1) - i[V_1(\rho_{e_1e_1}-\rho_{g_1g_1}) - V_p\rho_{g_2g_1}(\omega_1-\omega_p)], \tag{9}$$

$$\dot{\rho}_{e_2g_2}(\omega_2) = -(i\Delta_2+\Gamma/2+\gamma)\rho_{e_2g_2}(\omega_2) - i[V_2(\rho_{e_2e_2}-\rho_{g_2g_2}) + V_p\rho_{e_2e_1}(\omega_2-\omega_p)], \tag{10}$$

$$\dot{\rho}_{e_1g_2}(\omega_p) = -(i\Delta_p+\Gamma/2+\gamma)\rho_{e_1g_2}(\omega_p) - i[V_p(\rho_{e_1e_1}-\rho_{g_2g_2}) + V_2\rho_{e_1e_2}(\omega_p-\omega_2) - V_1\times\rho_{g_1g_2}(\omega_p-\omega_1)], \tag{11}$$

$$\dot{\rho}_{e_2g_1}(\omega_1+\omega_2-\omega_p) = -[i(\Delta_1+\Delta_2-\Delta_p)+\Gamma/2+\gamma]\times\rho_{e_2g_1}(\omega_1+\omega_2-\omega_p) - i[V_1\rho_{e_2e_1}(\omega_2-\omega_p) - V_2\rho_{g_2g_1}(\omega_1-\omega_p)], \tag{12}$$

$$\dot{\rho}_{e_1e_1} = -(\Gamma+\gamma)\rho_{e_1e_1} - i[V_1^*\rho_{e_1g_1}(\omega_1) - V_1\rho_{g_1e_1}(-\omega_1) + V_p^*\rho_{e_1g_2}(\omega_p) - V_p\rho_{g_2e_1}(-\omega_p)], \tag{13}$$

$$\dot{\rho}_{e_2e_2} = -(\Gamma+\gamma)\rho_{e_2e_2} - i[V_2^*\rho_{e_2g_2}(\omega_2) - V_2\rho_{g_2e_2}(-\omega_2)], \tag{14}$$

$$\dot{\rho}_{e_1e_2}(\omega_p-\omega_2) = -[i(\Delta_p-\Delta_2)+\Gamma+\gamma]\rho_{e_1e_2}(\omega_p-\omega_2) - i[V_2^*\rho_{e_1g_2}(\omega_p) - V_1\rho_{g_1e_2}(\omega_p-\omega_1-\omega_2) - V_p\rho_{g_2e_2}(-\omega_2)], \tag{15}$$

where $A=\sqrt{\mu_{e_1g_1}^2/(\mu_{e_1g_1}^2+\mu_{e_1g_2}^2)}$ and $B=\sqrt{\mu_{e_1g_2}^2/(\mu_{e_1g_1}^2+\mu_{e_1g_2}^2)}$ are the spontaneous decay rate branching ratios for the transitions between states e_1 and g_1, g_2, respectively, Γ is the total spontaneous emission rate from the excited state e_i to all the ground states, and γ is the rate of transfer to and from the reservoir due to time of flight of the atoms through the copropagating laser beams. The detunings $\Delta_{1,2,p}$ are defined as $\Delta_1=\omega_{e_1g_1}-\omega_1$, $\Delta_2=\omega_{e_2g_2}-\omega_2$, and $\Delta_p=\omega_{e_1g_2}-\omega_p$, and $\rho_{g_ig_i}^{eq}$ is the equilibrium population of state g_i, in the absence of any electromagnetic fields.

We note that the pump Rabi frequency we use when discussing realistic systems is the reduced Rabi frequency Ω which is related to the Rabi frequency of the individual transitions by the relation [13]

$$2V_{e_ig_j} = \frac{2\mu_{e_ig_j}E}{\hbar} = (-1)^{F_e-m_e}\begin{pmatrix} F_e & 1 & F_g \\ -m_e & q & m_g \end{pmatrix}\Omega, \tag{16}$$

where $\Omega=2\langle F_e\|\mu\|F_g\rangle E/\hbar$ [13] is the general pump Rabi frequency for the $F_e\rightarrow F_g$ transition. The N system we consider here is analogous to a degenerate transition with $F_e>F_g>0$, pumped by a resonant σ^+ polarized pump laser and probed by a tunable weak π polarized probe laser. In this case the ratio of the strengths of the $|F_g,m_g=F_g\rangle\rightarrow|F_e=F_g+1,m_e=F_g+1\rangle$ and the $|F_g,m_g=F_g-1\rangle\rightarrow|F_e=F_g+1,m_e=F_g\rangle$ transitions can be calculated from Eq. (16). Thus in order to compare the N system with such a degenerate system, we assume that a single pump interacts with both pumped transitions so that $V_1=AV_2$. The relative strength of V_1 and V_2 depends on the total angular momentum ($F_{g,e}$) of the ground and excited states coupled by the pump lasers, and are therefore different for different atomic transitions. However, the ratio $V_1/V_2=A$ does not vary much and therefore does not significantly affect the absorption curves. Thus a full analysis of this scheme for various ratios of the two pump lasers is not necessary.

The transfer of excited-state coherence to ground-state coherence which appears in Eq. (8) and in its complex conjugate, is multiplied by a parameter b, which can take any value between zero and one, as will be explained later in this paragraph. As we showed in a previous paper [9], there are two requirements for the existence of TOC. First, there must be a nonzero coherence between two populated excited states that occurs due to a two-photon transition between these states. This transition consists of either the absorption of a

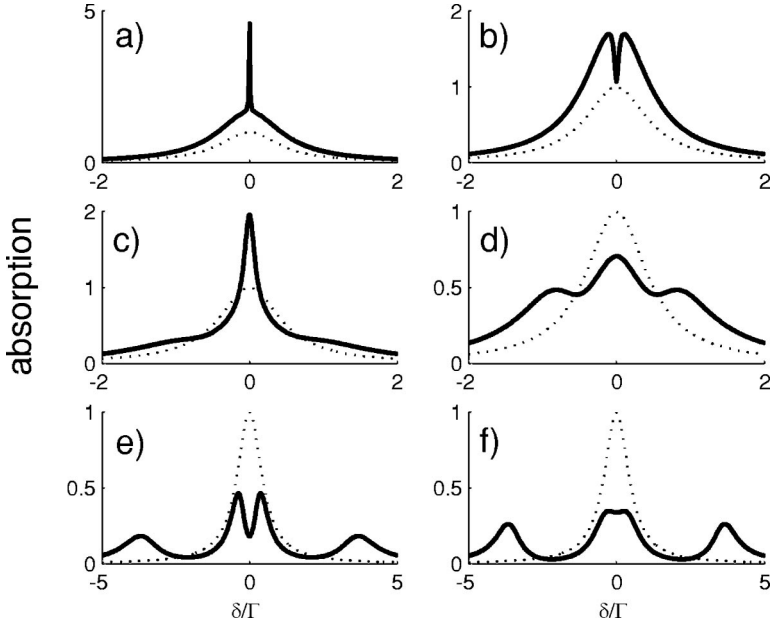

FIG. 2. Calculated probe absorption spectra, $\mathrm{Im}(\rho_{e_1g_2})\Gamma/V_p$, with $V_1=0.816V_2$ and $\gamma/\Gamma=0.001$. In the left column [(a), (c), and (e)] TOC is included and in the right column [(b), (d), and (f)] TOC is not included. The dotted curve is the probe absorption in the absence of pump lasers. In (a) and (b), $V_2/\Gamma=0.1$, in (c) and (d), $V_2/\Gamma=0.5$, and in (e) and (f), $V_2/\Gamma=2$.

pump photon and emission of a probe photon, or vice versa. It should be noted that excited state coherences can also exist due to the pump laser alone, for example, in the case where a σ pump interacts with a $F_e>F_g>0$ system, leading to the observation of EIA in the Hanle configuration [14]. The second requirement for obtaining TOC is the existence of ground state coherences that oscillate at the same frequencies as the excited state coherences. When both requirements are fulfilled, the excited state coherences decay to the ground state coherences via spontaneous emission. For closed (cycling) transitions, $b=1$. For open systems, $0<b<1$, since there, only part of the excited state population and coherence decays to an unpumped ground state. Consequently, EIA is not always observed in open systems [9]. When $b=0$ there is no TOC and our equations reduce to those of Dong *et al.* [10].

As we are only interested in steady-state results, we set the time derivatives of the Fourier amplitudes in Eqs. (6)–(15) to zero. The quantities we calculate are the probe absorption coefficient $\alpha(\omega_p)$ given by

$$\alpha(\omega_p)=\frac{4\pi\omega_p N|\mu_{e_1g_2}|^2}{cV_p\hbar}\mathrm{Im}[\rho_{e_1g_2}(\omega_p)], \tag{17}$$

and the probe refraction given by

$$n(\omega_p)-1=\frac{N|\mu_{e_1g_2}|^2}{V_p\hbar}\mathrm{Re}[\rho_{e_1g_2}(\omega_p)]. \tag{18}$$

The dispersion is the slope of the refraction with respect to the probe frequency.

We also calculate the Doppler broadened probe absorption or refraction, which is given by

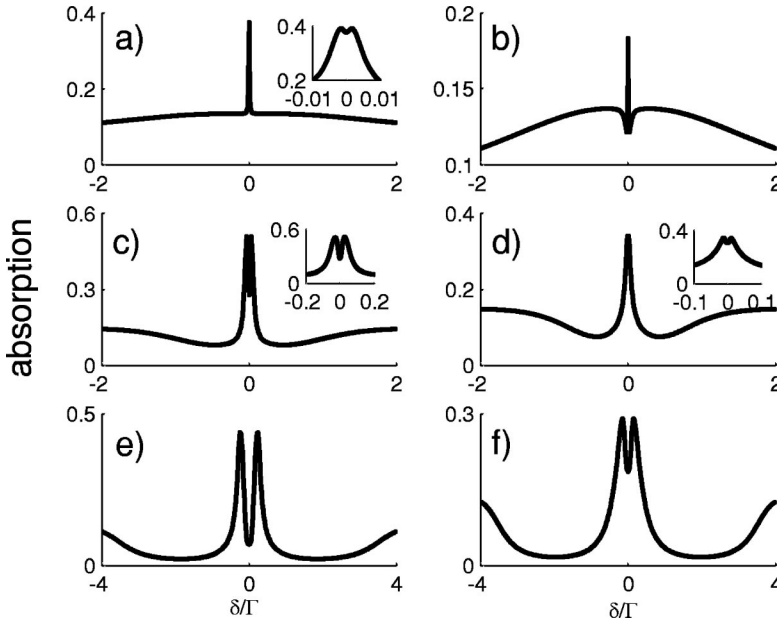

FIG. 3. Doppler broadened spectra for the same parameters as in Fig. 2. The Doppler width is $D/\Gamma=10$.

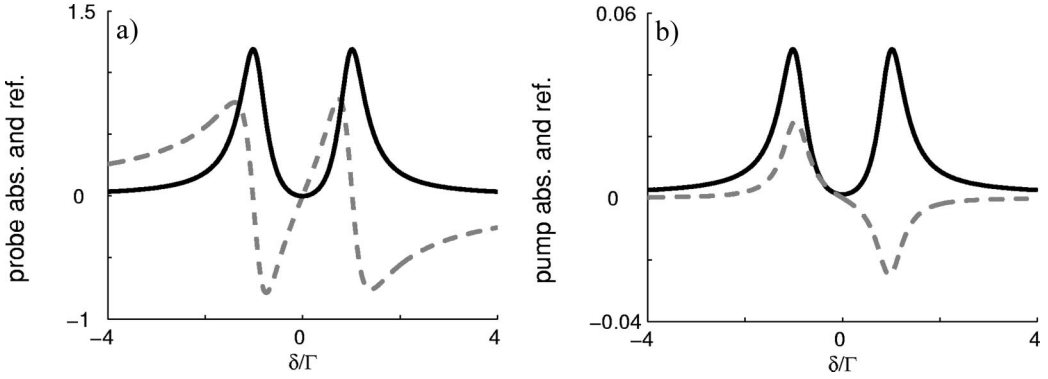

FIG. 4. Λ system interacting with a resonant pump: (a) calculated probe absorption, $\mathrm{Im}(\rho_{e_1g_2})\Gamma/V_p$ (solid line), and refraction, $\mathrm{Re}(\rho_{e_1g_2})\Gamma/V_p$ (dashed line); (b) calculated pump absorption, $\mathrm{Im}(\rho_{e_1g_1})\Gamma/V_1$ (solid line), and refraction, $\mathrm{Re}(\rho_{e_1g_1})\Gamma/V_1$ (dashed line). Parameters are $V_1/\Gamma=1$, $V_2=0$, $V_p/\Gamma=0.1$, and $\gamma/\Gamma=0.001$. The spectra are plotted as a function of δ/Γ.

$$q^D=(1/\pi D^2)^{1/2}\int_{-\infty}^{\infty} q(\Delta_1',\Delta_2',\Delta_p')\exp[-(\Delta_1-\Delta_1')^2/D^2]d\Delta_1', \tag{19}$$

where $q=\alpha(\omega_p)$ or $n(\omega_p)-1$, $\Delta_2'-\Delta_2\simeq\Delta_p'-\Delta_p\simeq\Delta_1'-\Delta_1$, and $D=(2k_BT/m)^{1/2}\omega_0/c$ is the Doppler width.

B. Probe absorption spectrum with and without TOC

In this section, we present numerical results obtained for resonant pump lasers and a tunable probe laser. We assume the excited and ground states to be degenerate so that both pumps have the same frequency $\omega_1=\omega_2=\omega_{eg}$. We plot all the spectra as a function of the dimensionless probe-pump detuning $\delta/\Gamma=(\omega_p-\omega_1)/\Gamma=-\Delta_p/\Gamma$. We compare the absorption spectra calculated using the N configuration model which includes TOC [$b=1$ in Eq. (8)], and leads to EIA, with those obtained from the same model in the absence of TOC ($b=0$) [10]. In Fig. 2 we present the probe absorption spectra with TOC (left column) and without TOC (right column), for various pump intensities. The background absorption of the probe laser in the absence of the pump lasers, which is independent of TOC, is plotted as dotted curves in Figs. 2(a)–2(f). We recall that in order to compare our results with a degenerate two-level system interacting with a single pump and probe, we take $V_1=AV_2$. We choose the values $A=0.816$ and $B=0.578$, which give the same branching ratios as obtained for the $|F_g=2,m_g=1\rangle\rightarrow|F_e=3,m_e=2\rangle$ and $|F_g=2,m_g=2\rangle\rightarrow|F_e=3,m_e=3\rangle$ transitions in the D_2 line of ^{87}Rb. The Rabi splittings of the N configuration atom due to the pump lasers are shown in Fig. 1. The probe laser sees four different dressed states and therefore we expect to find four absorption peaks at $\pm(V_1\pm V_2)$. At low pump intensities these peaks are not resolved and the probe absorption displays EIA in the presence of TOC [Fig. 2(a)] and a dip at line center in its absence [Fig. 2(b)]. These results agree with previous calculations by Taichenachev *et al.* [7]. As the pump intensity increases the EIA peak height decreases [Fig. 2(c)], and the dip for the case without TOC disappears [Fig. 2(d)], and then reappears when the pump is further increased [Fig. 2(f)]. In addition, absorption sidebands due to the Rabi

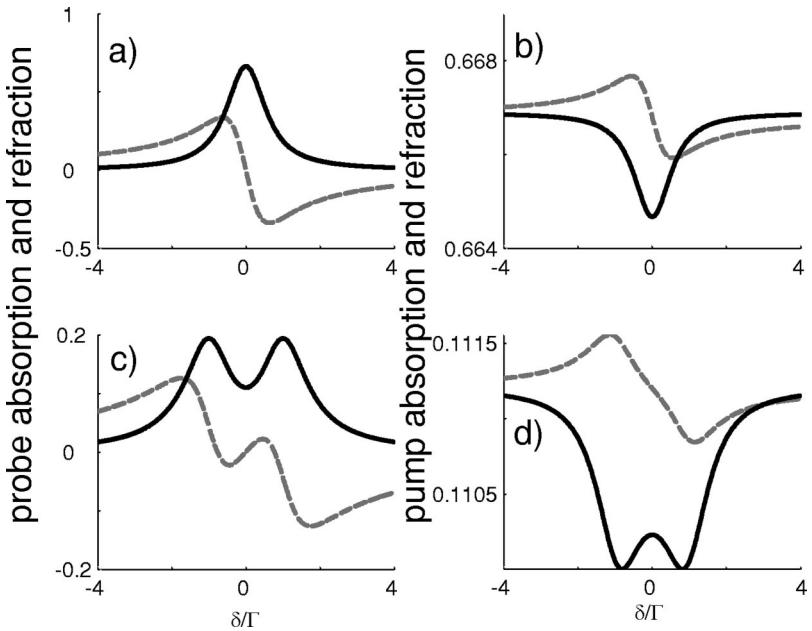

FIG. 5. *V* system interacting with a resonant pump: (a) and (c), calculated probe absorption, $\mathrm{Im}(\rho_{e_1g_2})\Gamma/V_p$ (solid line), and refraction, $\mathrm{Re}(\rho_{e_1g_2})\Gamma/V_p$ (dashed line); (b) and (d), calculated pump absorption, $\mathrm{Im}(\rho_{e_2g_2})\Gamma/V_2$ (solid line), and refraction, $\mathrm{Re}(\rho_{e_2g_2})\Gamma/V_2$ (dashed line). Parameters for (a) and (b) are $V_1=0$, $V_2/\Gamma=0.25$ and $V_p/\Gamma=0.025$, and for (c) and (d), $V_1=0$, $V_2/\Gamma=1$ and $V_p/\Gamma=0.1$. $\gamma/\Gamma=0.001$ for all cases. For clarity, the refractions in (b) and (d) which are centered at zero, have been shifted upwards. In addition the refraction in (d) has been divided by 10.

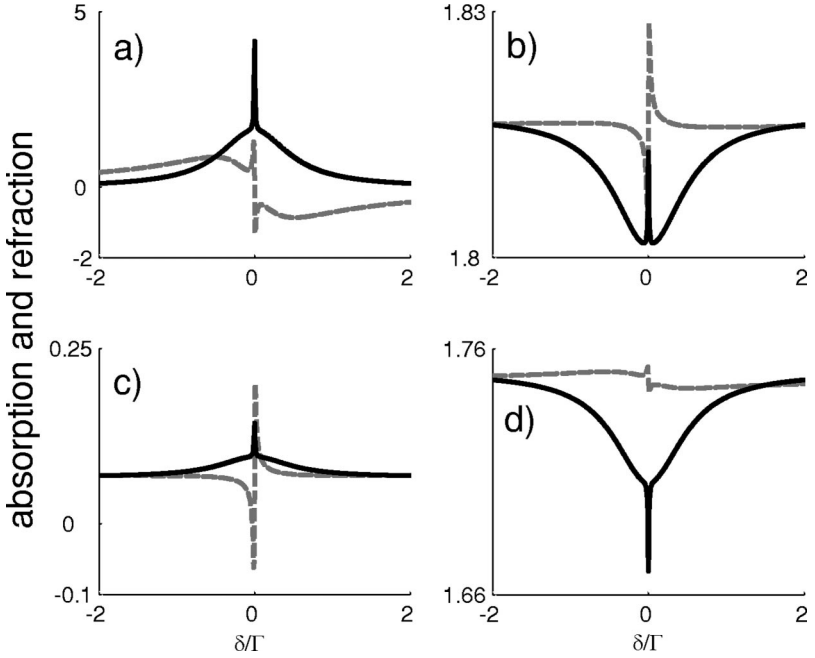

FIG. 6. *N* system interacting with two resonant pumps: (a) calculated probe absorption, $\mathrm{Im}(\rho_{e_1g_2})\Gamma/V_p$ (solid line) and refraction, $\mathrm{Re}(\rho_{e_1g_2})\Gamma/V_p$ (dashed line); (b) calculated pump absorption, $\Gamma[\mathrm{Im}(\rho_{e_1g_1})A^2/V_1+\mathrm{Im}(\rho_{e_2g_2})/V_2]$ (solid line) and refraction, $\Gamma[\mathrm{Re}(\rho_{e_1g_1})A^2/V_1+\mathrm{Re}(\rho_{e_2g_2})/V_2]$ (dashed line); (c) real (solid line) and imaginary (dashed line) parts of $(\rho_{e_1g_1})\Gamma A^2/V_1$, and (d) real (solid line) and imaginary (dashed line) parts of $\mathrm{Im}(\rho_{e_2g_2})\Gamma/V_2$. Parameters are $V_2/\Gamma=0.1$, $V_p/\Gamma=0.01$, $A=0.816$, and $\gamma/\Gamma=0.001$. For clarity, the refractions in (b), (c), and (d), which are centered at zero, have been shifted upwards. In addition the refraction in (c) and (d) have been multiplied by 10.

splitting develop at $\pm(V_1+V_2)$. When $V_2/\Gamma=2$, all four peaks are resolved in the spectra, both in the presence and the absence of TOC [see Figs. 2(e) and 2(f)]. It is interesting to note that in addition to generating EIA, TOC has three other effects on the absorption spectra which can be seen by comparing Figs. 2(e) and 2(f). First, when TOC is included, the center peak develops a dip at a lower pump intensity and this dip is deeper than in the absence of TOC. Second, the absorption near line center is higher, and third, the absorption in the sidebands is lower than in the case without TOC. It should be noted that the behavior of the *N* configuration with TOC, namely the decrease in the EIA with increasing pump intensity and the development of a dip at line center at even higher intensities also exists in the EIA spectra obtained in the Hanle configuration [14].

In order to understand the influence of TOC on the absorption spectra we have developed an analytical expression for the probe absorption that clearly shows the effect of TOC (see the Appendix).

C. Doppler-broadened probe absorption spectrum

When Doppler broadening is included, the spectra shown in Fig. 2 are replaced by those of Fig. 3. At low intensity in the presence of TOC [Fig. 3(a)], the EIA peak develops a dip, as described by Taichenachev *et al.* [8]. The dip in the spectrum calculated without TOC [Fig. 2(b)] becomes a peak on top of the Doppler-broadened absorption curve [Fig. 3(b)]. This result has not been noted in previous publications. In order to explain its origin, it should be noted that the

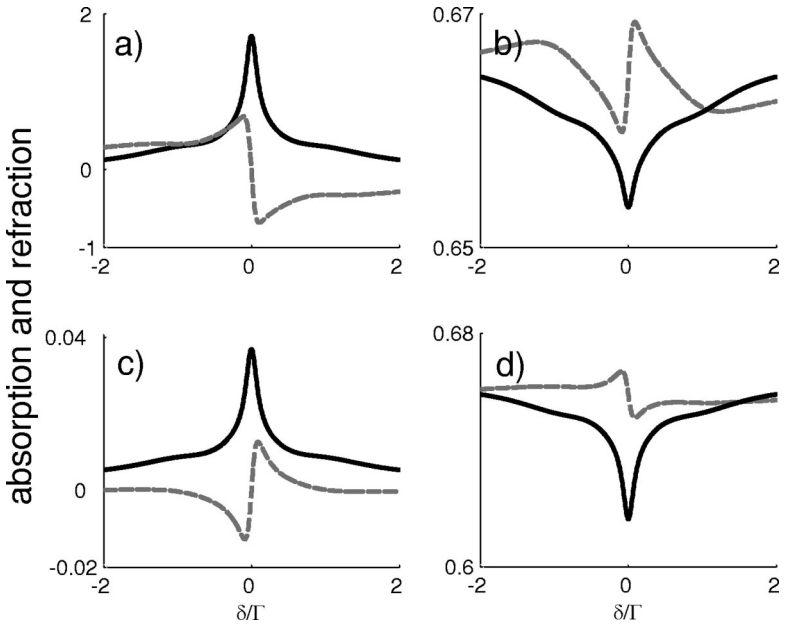

FIG. 7. *N*-system interacting with two resonant pumps: (a) calculated probe absorption, $\mathrm{Im}(\rho_{e_1g_2})\Gamma/V_p$ (solid line) and refraction, $\mathrm{Re}(\rho_{e_1g_2})\Gamma/V_p$ (dashed line); (b) calculated pump absorption, $\Gamma[\mathrm{Im}(\rho_{e_1g_1})A^2/V_1+\mathrm{Im}(\rho_{e_2g_2})/V_2]$ (solid line) and refraction, $\Gamma[\mathrm{Re}(\rho_{e_1g_1})A^2/V_1+\mathrm{Re}(\rho_{e_2g_2})/V_2]$ (dashed line); (c) real (solid line) and imaginary (dashed line) parts of $(\rho_{e_1g_1})\Gamma A^2/V_1$, and (d) real (solid line) and imaginary (dashed line) parts of $\mathrm{Im}(\rho_{e_2g_2})\Gamma/V_2$. Parameters are $V_2/\Gamma=0.5$, $V_p/\Gamma=0.05$, $A=0.816$ and $\gamma/\Gamma=0.001$. For clarity, the refractions in (b) and (d), which are centered at zero, have been shifted upwards.

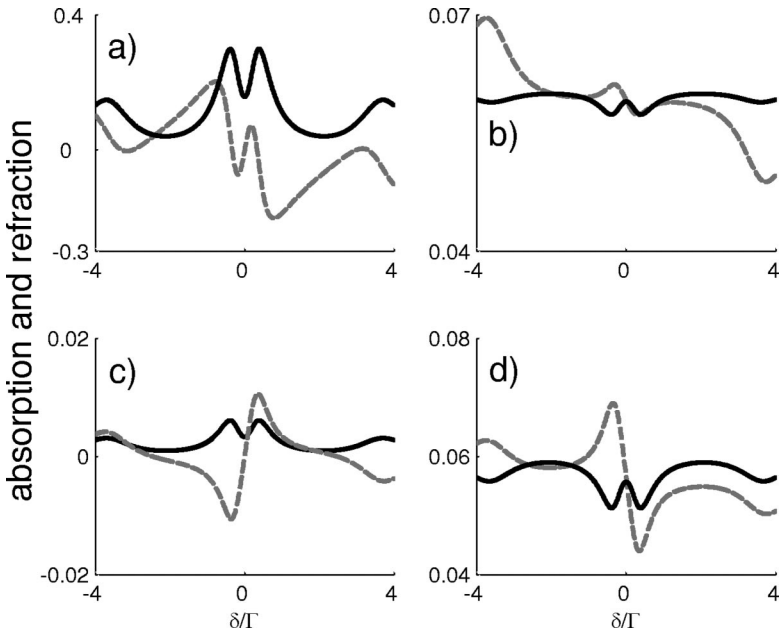

FIG. 8. *N* system interacting with two resonant pumps: (a) calculated probe absorption, $\mathrm{Im}(\rho_{e_1g_2})\Gamma/V_p$ (solid line) and refraction, $\mathrm{Re}(\rho_{e_1g_2})\Gamma/V_p$; (b) calculated pump absorption, $\Gamma[\mathrm{Im}(\rho_{e_1g_1})A^2/V_1+\mathrm{Im}(\rho_{e_2g_2})/V_2]$ (solid line) and refraction, $\Gamma[\mathrm{Re}(\rho_{e_1g_1})A^2/V_1+\mathrm{Re}(\rho_{e_2g_2})/V_2]$ (dashed line); (c) real (solid line) and imaginary (dashed line) parts of $(\rho_{e_1g_1})\Gamma A^2/V_1$, and (d) real (solid line) and imaginary (dashed line) parts of $\mathrm{Im}(\rho_{e_2g_2})\Gamma/V_2$. Parameters are $V_2/\Gamma=2$, $V_p/\Gamma=0.2$, $A=0.816$, and $\gamma/\Gamma=0.001$. For clarity, the refractions in (b) and (d), which are centered at zero, have been shifted upwards.

Doppler-broadened spectrum derives from interference between the contributions to the spectrum from different pump detunings [see Eq. (19)]. When the pump detuning is nonzero, the absorption spectrum near $\delta=0$ has a dispersive shape which is centered *near* (but not exactly at) $\delta=0$, as is the case for a simple two-level system [15,16]. These contributions interfere to give the peak. At moderate intensity, the dips appear at the center of the absorption lines [Figs. 3(c) and 3(d)], both in the presence and the absence [10] of TOC. These dips are enhanced at higher intensities [Figs. 3(e) and 3(f)]. An important point to note is that the whole central feature, with or without a dip, becomes *narrower* as the Doppler width increases [8]. This effect is analogous to the Doppler narrowing of the electromagnetically induced transparency (EIT) window in a Λ system which has been both predicted [17,18] and observed [19]. The changes in the spectra on Doppler broadening can be understood by analyzing the contributions of the various velocity groups to the Doppler integral.

III. ABSORPTION AND REFRACTION OF A RESONANT PUMP LASER AS A FUNCTION OF THE PROBE DETUNING

In this section we solve the full set of equations, given in Eqs. (6)–(15), in order to show the effect of a probe on the pump absorption and refraction. Such spectra have been measured for the Λ system by Müller *et al.* [20,21]. In order to understand the results for the *N* configuration we must first review the three-level Λ and *V* systems (see Ref. [22]).

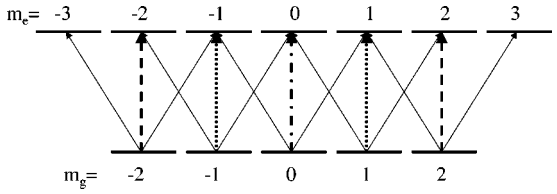

FIG. 9. Energy-level scheme for the $F_g=2\rightarrow F_e=3$ transition interacting with a σ polarized resonant pump laser and a tunable π polarized probe laser.

A. Λ system

The probe and pump absorption and refraction for the Λ system are obtained from Eqs. (6)–(15) by setting $V_2=0$. As seen in Figs. 4(a) and 4(b), the probe and pump absorption spectra both display EIT. This EIT persists for all pump intensities [20,21]. However, the probe dispersion is positive whereas the pump dispersion is negative.

B. *V* system

The *V* system is obtained by setting $V_1=0$, $A=0$ and $B=1$ in Eq. (6)–(15). The probe and pump absorption and refraction are plotted in Fig. 5. For low pump intensities the probe absorption spectrum is characterized by a peak at line center, whereas the pump absorption is characterized by a dip, both accompanied by negative dispersion [Figs. 5(a) and 5(b)]. When the pump intensity increases the probe absorption spectrum splits into two Autler-Townes peaks which are accompanied by positive dispersion [Fig. 5(c)], whereas the pump intensity has two dips due to the Autler-Townes effect and displays negative dispersion [Fig. 5(d)].

C. *N* configuration

Here, we investigate the pump absorption and refraction in the *N* system, as the probe laser frequency is swept through resonance. The pump induces two transitions in the system (see Fig. 1) so that the pump absorption and refraction derive from both these transitions [23]. Thus, the pump absorption and refraction are proportional to the imaginary and real parts of $\rho_{e_1g_1}A^2/V_1+\rho_{e_2g_2}/V_2$ and the final spectra (see Figs. 6–8) are the result of competition between both

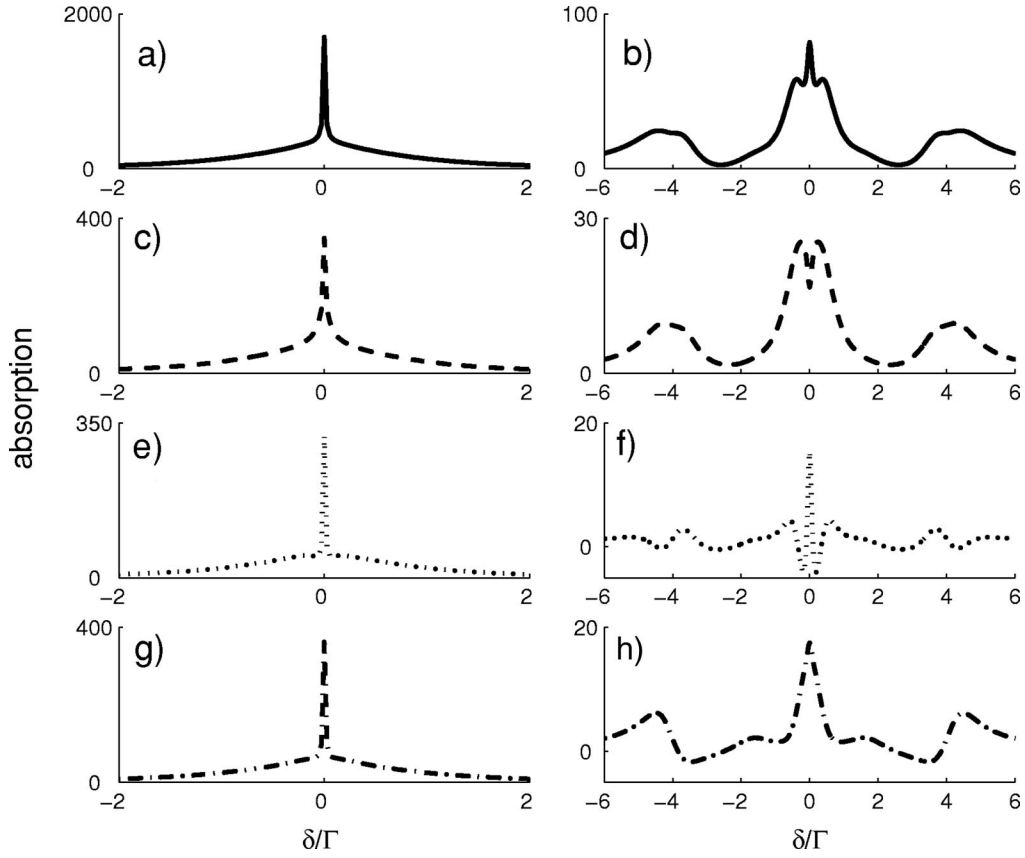

FIG. 10. Realistic atomic system: probe absorption for the cycling $F_g=2\rightarrow F_e=3$ transition of the D_2 line in ^{87}Rb, interacting with a σ polarized resonant pump laser and a tunable π polarized probe laser, with (a) $\Omega/\Gamma=2$, and (b) $\Omega/\Gamma=15$. In (c), (e), and (g) and in (d), (f), and (h), we plot the individual contributions to the absorption of (a) and (b), respectively, marked the same way as in Fig. 9. The atomic density was taken to be 10^{12} atoms/cm^3 and $\gamma/\Gamma=0.001$.

contributions. The contribution to the absorption from the $g_1\rightarrow e_1$ transition has the same shape as the probe absorption, as is the case for the pump absorption in the Λ system (Fig. 4). In addition, the contribution from this transition to the refraction at line center has positive dispersion. The contribution from $g_2\rightarrow e_2$ transition has the opposite shape to the probe absorption as in the two-level system [12], and is accompanied by negative dispersion, which is also the case for the V system. It should be emphasized that both contributions to the pump absorption are important, even when their average magnitudes differ by an order of magnitude, since the variation of the absorption due to the change in δ, can be of the same magnitude.

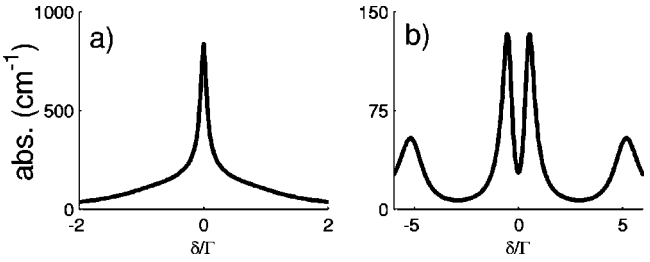

FIG. 11. Realistic atomic system: probe absorption for the cycling $F_g=2\rightarrow F_e=3$ transition, of the D_2 line in ^{87}Rb, interacting with a σ^+ polarized resonant pump laser and a tunable π polarized probe laser, with (a) $\Omega/\Gamma=2$, and (b) $\Omega/\Gamma=15$. The atomic density was taken to be 10^{12} atoms/cm^3 and $\gamma/\Gamma=0.001$.

At low pump intensities, where the probe spectrum is characterized by EIA [Fig. 6(a)], the pump absorption [Fig. 6(b)] also has an EIA peak, contributed by the $g_1\rightarrow e_1$ transition [Fig. 6(c)], inside a dip contributed by the $g_2\rightarrow e_2$ transition [Fig. 6(d)]. As the pump intensity increases, the population is optically pumped into the g_2 and e_2 states and the EIA peak in the probe absorption decreases in intensity [compare Fig. 7(a) with Fig. 6(a)]. The pump absorption peak disappears and the absorption decreases [compare Fig. 7(b) with Fig. 6(b)] with the contribution from the $g_2\rightarrow e_2$ transition dominating that from the $g_1\rightarrow e_1$ transition [see Figs. 7(c) and 7(d)]. The dispersion at line center remains positive since the dominant contribution comes from the $g_1\rightarrow e_1$ transition [Fig. 7(b)]. At even higher pump intensities, the probe absorption splits into two pairs of Autler-Townes peaks [Fig. 8(a)]. The total pump absorption and refraction [Fig. 8(b)] for this case is dominated by the $g_2\rightarrow e_2$ transition [compare Figs. 8(c) and 8(d)]. At these intensities, the pump dispersion becomes negative [Fig. 8(b)].

IV. APPLICATION TO ATOMIC SYSTEMS

Most experiments where EIA is observed are performed with pump and probe lasers whose polarizations are linear and perpendicular to each other, interacting with a closed $F_g \rightarrow F_e = F_g + 1$ transition. An example of such systems is the $F_g = 2 \rightarrow F_e = 3$ in the D_2 line of ^{87}Rb, interacting with a resonant σ polarized pump laser and a tunable π polarized probe laser (see Fig. 9). We calculate the spectra for this configuration by solving the Bloch equations for a degenerate two-level system, interacting with a pump and weak probe, discussed in our previous publications [9,24]. As shown in Figs. 10(a) and 10(b), the EIA peak, found at low pump intensity for this system, persists even when the pump intensity is high. For the same atomic transition, but with the σ polarized pump replaced by one with σ^+ polarization, the EIA peak develops a dip at line center with increasing pump intensity, as shown in Figs. 11(a) and 11(b). As expected, this behavior resembles that of an *N* system [see Figs. 2(a) and 2(e)]. The reason that the probe absorption spectrum, in the case of the σ polarized pump, does not split at high pump intensity can be found by considering the separate contributions to the spectrum. From Fig. 9, we see that due to symmetry, there are three distinct probe transitions that contribute to the total spectrum. The only probe transitions that participate in *N*-like systems are the $m_g = |2| \rightarrow m_e = |2|$ transitions, as can be seen from their contributions to the total spectrum shown in Figs. 10(c) and 10(d). The other probe transitions, $m_g = |1|, 0 \rightarrow m_e = |1|, 0$, each participate in two overlapping *N*-like systems. At low intensity, their contributions to the total spectrum shown in Figs. 10(e) and 10(g) display EIA peaks, which persist even at higher intensity, thereby masking the dip contributed by the *N*-like system. Only at experimentally unreasonable intensities is a dip obtained. This explains the fact that splitting in the absence of Doppler broadening has not been observed for the case of linear, perpendicularly polarized lasers.

It should be pointed out that Kim *et al.* [6] has shown experimentally that when the pump laser is σ polarized, a dip develops at line center on Doppler broadening. This dip should be distinguished from that expected in the absence of Doppler broadening.

V. CONCLUSIONS

We have investigated the four-level *N* configuration both analytically and numerically, for various pump and probe intensities, with and without TOC, and compared the results obtained to those of realistic atomic systems. We find that TOC affects the whole spectrum, not just the EIA peak. We show that the EIA peak splits as the pump intensity increases, even in absence of Doppler broadening. When Doppler broadening is included, we reproduce the results previously reported [8,10]. At low pump intensity, and in the absence of TOC, we find that the dip that occurs in the absence of Doppler broadening is transformed into a peak by Doppler broadening. We also discuss the influence of the probe on the pump absorption and refraction and find that both the pump and probe show EIA peaks when the pump intensity is low, and complementary behavior when the pump is intense. At both low and high pump intensity, the pump and probe dispersions are of opposite sign.

We compare the results with those of realistic systems. When the pump is σ^+ polarized and the probe is π polarized, the results are similar to those of the *N* configuration, in that a dip can be obtained at line center even in the absence of Doppler broadening. However this dip does not occur at reasonable pump intensities when the pump laser is σ polarized. This can be explained by considering the separate contributions to the probe absorption.

ACKNOWLEDGMENTS

We wish to thank Dr. R.-H. Rinkleff and L. Spani Molella for their hospitality and stimulating discussions.

APPENDIX: ANALYSIS OF THE ROLE OF TOC

We develop an analytical expression for the probe absorption in the *N* system. In order to compare the *N* system with realistic systems, we assume that a single resonant pump interacts with both pumped transitions and set $V_1 = AV_2$ and $\Delta_1 = \Delta_2 = 0$ in Eqs. (6)–(15). By inserting Eqs. (9), (11), and (12) into Eq. (8), and Eqs. (10)–(12) into Eq. (15), we obtain the following set of linear equations for the ground- and excited-state coherences:

$$D_g \rho_{g_1 g_2} = A_g + B_g \rho_{e_1 e_2}, \tag{A1}$$

$$D_e \rho_{e_1 e_2} = A_e + B_e \rho_{g_1 g_2}, \tag{A2}$$

where

$$A_g = AV_2 V_p \left(\frac{\rho_{e_1 e_1} - \rho_{g_1 g_1}}{\Gamma/2 + \gamma} - \frac{\rho_{e_1 e_1} - \rho_{g_2 g_2}}{i\Delta_p + \Gamma/2 + \gamma} \right), \tag{A3}$$

$$B_g = \frac{2AV_2^2}{i\Delta_p + \Gamma/2 + \gamma} + bA\Gamma, \tag{A4}$$

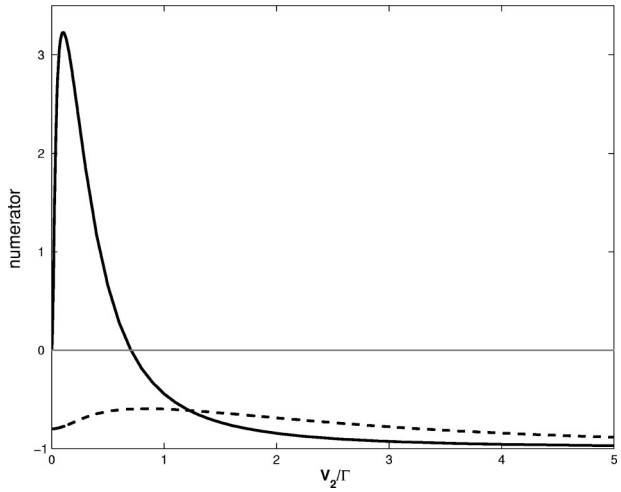

FIG. 12. The numerator of the second term of Eq. (A9) as a function of increasing V_2, with (solid line) and without (dashed line) TOC. When the numerator is positive, EIA occurs.

$$D_g = i\Delta_p + \gamma + \frac{V_p^2}{\Gamma/2+\gamma} + \frac{V_2^2(1+A^2)}{i\Delta_p + \Gamma/2 + \gamma}, \tag{A5}$$

$$A_e = V_2 V_p \left(\frac{\rho_{g_2 g_2} - \rho_{e_2 e_2}}{\Gamma/2+\gamma} + \frac{\rho_{g_2 g_2} - \rho_{e_1 e_1}}{i\Delta_p + \Gamma/2 + \gamma} \right), \tag{A6}$$

$$B_e = \frac{2AV_2^2}{i\Delta_p + \Gamma/2 + \gamma}, \tag{A7}$$

$$D_e = i\Delta_p + \Gamma + \gamma + \frac{V_p^2}{\Gamma/2+\gamma} + \frac{V_2^2(1+A^2)}{i\Delta_p + \Gamma/2 + \gamma}. \tag{A8}$$

We now solve Eqs. (A1) and (A2) in order to obtain analytical expressions for the ground and excited state coherences. These expressions are then inserted into the expression for $\rho_{e_1 g_2}$ in Eq. (11), whose imaginary part is proportional to the probe absorption:

$$\begin{aligned}\rho_{e_1 g_2}(\omega_p) &= \frac{-[V_p(\rho_{e_1 e_1} - \rho_{g_2 g_2}) + V_2 \rho_{e_1 e_2}(\omega_p - \omega_2) - V_1 \rho_{g_1 g_2}(\omega_p - \omega_1)]}{\Delta_p - i(\Gamma/2+\gamma)} \\ &= -\frac{V_p(\rho_{e_1 e_1} - \rho_{g_2 g_2})}{\Delta_p - i(\Gamma/2+\gamma)} - \frac{V_2 \frac{A_e}{D_e} + \left(V_2 \frac{B_e}{D_e} - V_1 \right) \left(-\frac{A_e}{B_e} + \frac{A_g D_e + \frac{D_e D_g A_e}{B_e}}{D_e D_g - B_e B_g} \right)}{\Delta_p - i(\Gamma/2+\gamma)}.\end{aligned} \tag{A9}$$

The first term in Eq. (A9) gives the background absorption of a two-level system interacting with only a probe laser, and the second term is the change in the background absorption induced by the pump lasers. In Fig. 12, we plot the numerator of the second term, at $\Delta_p = 0$, as a function of increasing pump intensity, both with and without TOC. We note that EIA is obtained when the numerator of this term is positive. It can thus be clearly seen from Fig. 12 that EIA is only obtained when TOC is included and, in addition, the pump Rabi frequency is low.

In order to explain the effect of TOC on the absorption, let us consider the case of a weak probe. For this case Eqs. (6)–(15) can be solved in two stages. In the first stage, only interaction with the strong pump lasers is considered. This gives us the pump-induced coherences and populations which are then inserted into Eqs. (A4)–(A8). In the second stage, the probe which together with the pump produces TOC, is introduced into the problem. Thus, the only difference between the case which includes TOC and the case which does not is the value of B_g. At line center, where $\Delta_p = 0$, the absolute value of B_g is larger when TOC is included, leading to a smaller value of the denominator $D_e D_g - B_e B_g$. As a result $(A_g D_e + D_e D_g A_e / B_e)/(D_e D_g - B_e B_g)$ becomes bigger than A_e / B_e making the second term in Eq. (A9) positive for low pump intensities. For high pump intensities the numerator is more negative when TOC is included, resulting in a larger dip at line center.

[1] A. Lezama, S. Barreiro, and A. M. Akulshin, Phys. Rev. A **59**, 4732 (1999).

[2] A. Lipsich, S. Barreiro, A. M. Akulshin, and A. Lezama, Phys. Rev. A **61**, 053803 (2000).

[3] Y. Dancheva, G. Alzetta, S. Cartaleva, M. Taslakov, and C. Andreeva, Opt. Commun. **178**, 103 (2000).

[4] C. Andreeva, S. Cartaleva, Y. Dancheva, V. Biancalana, A. Burchianti, C. Marinelli, E. Mariotti, L. Moi, and K. Nasyrov, Phys. Rev. A **66**, 012502 (2002).

[5] M. Kwon, K. Kyoungdae, H. S. Moon, H. D. Park, and J. B. Kim, J. Phys. B **34**, 2951 (2001).

[6] K. Kim, M. Kwon, H. D. Park, H. S. Moon, H. S. Rawat, K. An, and J. B. Kim, J. Phys. B **34**, 4801 (2001).

[7] A. V. Taichenachev, A. M. Tumaikin, and V. I. Yudin, Phys. Rev. A **61**, 011802(R) (1999).

[8] A. V. Taichenachev, A. M. Tumaikin, and V. Yudin, JETP Lett. **69**, 819 (1999).

[9] C. Goren, A. D. Wilson-Gordon, M. Rosenbluh, and H. Friedmann, Phys. Rev. A **67**, 033807 (2003).

[10] P. Dong, A. K. Popov, S. H. Tang, and J. Y. Gao, Opt. Commun. **188**, 99 (2001).

[11] A. M. Akulshin, S. Barreiro, and A. Lezama, Phys. Rev. Lett. **83**, 4277 (1999).

[12] H. Friedmann and A. D. Wilson-Gordon, Phys. Rev. A **36**, 1333 (1987).

[13] A. R. Edmonds, *Angular Momentum in Quantum Mechanics* (Princeton University Press, Princeton, 1960).

[14] F. Renzoni, C. Zimmermann, P. Verkerk, and E. Arimondo, J. Opt. B: Quantum Semiclassical Opt. **3**, S7 (2001).

[15] H. Friedmann and A. D. Wilson-Gordon, *Methods of Laser Spectroscopy* (Plenum, New York, 1986), p. 307

[16] G. Grynberg and C. Cohen-Tannoujdi, Opt. Commun. **96**, 150

(1993).
[17] A. V. Taichenachev, A. M. Tumaikin, and V. Yudin, JETP Lett. **72**, 119 (2000).
[18] A. Javan, O. Kocharovskaya, H. Lee, and M. O. Scully, Phys. Rev. A **66**, 013805 (2002).
[19] C. Ye and A. Zibrov, Phys. Rev. A **65**, 023806 (2002).
[20] M. Muller, F. Homann, R. H. Rinkleff, A. Wicht, and K. Danzmann, Phys. Rev. A **62**, 060501 (2000).
[21] M. Muller, F. Homann, R. H. Rinkleff, A. Wicht, and K. Danzmann, Phys. Rev. A **64**, 013803 (2001).
[22] A. Wicht, R. H. Rinkleff, L. S. Molella, and K. Danzmann, Phys. Rev. A **66**, 063815 (2002).
[23] S. Menon and G. S. Agarwal, Phys. Rev. A **59**, 740 (1999).
[24] C. Goren, A. D. Wilson-Gordon, M. Rosenbluh, and H. Friedmann, Phys. Rev. A **68**, 043818 (2003).